Development 136, 2933-2944 (2009) doi:10.1242/dev.040204

The *C. elegans* Tailless/TLX transcription factor *nhr-67* controls neuronal identity and left/right asymmetric fate diversification

Sumeet Sarin, Celia Antonio, Baris Tursun and Oliver Hobert*

An understanding of the molecular mechanisms of cell fate determination in the nervous system requires the elucidation of transcriptional regulatory programs that ultimately control neuron-type-specific gene expression profiles. We show here that the *C. elegans* Tailless/TLX-type, orphan nuclear receptor NHR-67 acts at several distinct steps to determine the identity and subsequent left/right (L/R) asymmetric subtype diversification of a class of gustatory neurons, the ASE neurons. *nhr-67* controls several broad aspects of sensory neuron development and, in addition, triggers the expression of a sensory neuron-type-specific selector gene, *che-1*, which encodes a zinc-finger transcription factor. Subsequent to its induction of overall ASE fate, *nhr-67* diversifies the fate of the two ASE neurons ASEL and ASER across the L/R axis by promoting ASER and inhibiting ASEL fate. This function is achieved through direct expression activation by *nhr-67* of the Nkx6-type homeobox gene *cog-1*, an inducer of ASER fate, that is inhibited in ASEL through the miRNA *lsy-6*. Besides controlling bilateral and asymmetric aspects of ASE development, *nhr-67* is also required for many other neurons of diverse lineage history and function to appropriately differentiate, illustrating the broad and diverse use of this type of transcription factor in neuronal development.

KEY WORDS: *C. elegans*, Left/right asymmetry, Neuronal development, Transcriptional regulation

INTRODUCTION

In acquiring a specific identity, a neuron must interpret spatial, temporal and lineal information throughout its development, from its birth as a neural precursor until its postmitotic state. The ASE chemosensory neurons of the nematode *C. elegans* have proven to be a useful system with which to study the regulatory mechanisms that define neuronal identity (Hobert, 2005; Hobert, 2006). The identity of the ASE neuron class can be broken down into individual components, which are controlled by distinct regulatory programs. ASE neurons express pan-neuronal features, shared by all neurons; they also express features that are specific to all sensory neurons and they express features that assign a unique identity to ASE. The unique identity determinant of ASE fate is the terminal selector gene *che-1* (Chang et al., 2003; Etchberger et al., 2007; Uchida et al., 2003). Its loss results in a failure to express ASE-specific features, but leaves expression of pan-sensory and pan-neuronal features intact. The RFX-box transcription factor *daf-19* controls pan-sensory features of ASE and all other sensory neurons (Swoboda et al., 2000). As yet unknown regulatory factors may act through a common cis-regulatory motif to control the expression of pan-neuronal features of a neuron (Ruvinsky et al., 2007). Whether and to what extent these regulatory programs are coupled to one another is not known.

After adoption of their initial, bilaterally symmetric identity, the ASE neurons undergo an additional diversification program that occurs across the L/R axis, the least understood axis during nervous system development. This diversification program results in the L/R asymmetric expression of a family of putative chemoreceptors of the guanylyl cyclase (*gcy*) family, with some *gcy* genes being exclusively and stereotypically expressed in ASEL and others in ASER (Ortiz et al., 2006; Yu et al., 1997). This molecular asymmetry endows the left and right ASE neuron with the ability to sense and discriminate a distinct set of chemosensory cues (Ortiz et al., 2009; Pierce-Shimomura et al., 2001; Suzuki et al., 2008). The L/R asymmetric gene expression program of ASEL and ASER is brought about by a complex gene regulatory network of several transcription factors and miRNAs that act in a bistable feedback loop (Fig. 1) (Hobert, 2006). This loop provides a transcriptional output that feeds into *gcy* gene expression. The input into the loop that determines which loop components predominate in ASEL versus ASER is not molecularly known, but is dependent on the distinct lineage history of the two ASE neurons and a Notch signal received differentially by the precursors of ASEL and ASER (Poole and Hobert, 2006).

In order to uncover additional components of this L/R asymmetric gene regulatory program, we undertook a large-scale genetic screen in which the ASE L/R fate decision was inappropriately executed (Sarin et al., 2007). One mutant locus isolated from this screen, *lsy-9*, displays a highly unusual phenotype. In what appears to be an intriguing reversal of asymmetry, a fraction of animals express the left fate marker *lim-6::gfp* exclusively in the ASER rather than the ASEL neuron (Sarin et al., 2007). No other such 'reversal' mutant was retrieved from the screen. In addition to the 'reversal' category, some animals also display a complete loss of the ASEL marker, whereas others display a 'bilateralization', in that both ASEL and ASER express the left fate marker (Sarin et al., 2007). Here, we describe this mutant phenotype in more detail and show that this gene is allelic to the orphan nuclear receptor encoding gene *nhr-67*, a homolog of *Drosophila* tailless, previously identified by genome sequence analysis (Sluder et al., 1999). We find that the unusual *nhr-67/lsy-9* phenotype is caused by two independent activities of *nhr-67* early and late in ASE development. We also show that *nhr-67* function controls the identity of various different neuronal cell types.

Howard Hughes Medical Institute, Department of Biochemistry and Molecular Biophysics, Columbia University Medical Center, 701 W.168th Street, New York, NY 10032, USA.

*Author for correspondence (or38@columbia.edu)

Accepted 30 June 2009

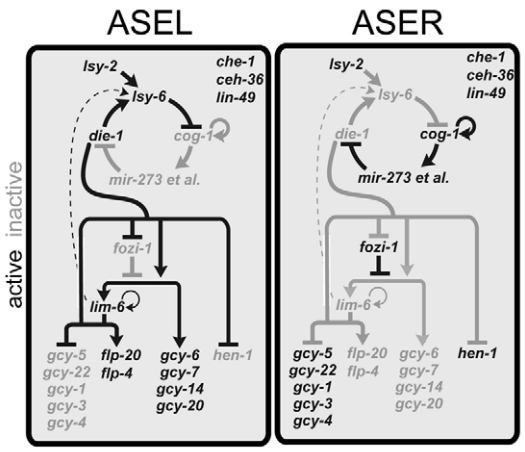

Fig. 1. Gene regulatory mechanisms that control ASEL/R development in *C. elegans*. ASEL and ASER fate are controlled by a bistable, double-negative feedback loop. All genes shown here are also directly controlled by the terminal selector gene *che-1*, an overall ASE fate inducer.

MATERIALS AND METHODS

Strains and transgenes

N2 Bristol wild-type (Brenner, 1974) and CB4856 Hawaiian wild-type (Hodgkin and Doniach, 1997) isolates were used. Transgenes that label ASEL and ASER fates included: ASEL markers *otIs3*V=Is[*gcy-7^{prom}::GFP; lin-15* (+)], *otIs114*I=Is[*lim-6^{prom}::gfp; rol-6(d)*] and *otIs160*IV=Is[*lsy-6^{prom}::gfp; unc-122^{prom}::GFP*]; ASER markers *ntIs1*V=Is[*gcy-5^{prom}::GFP; lin-15 (+)*] and *syIs73* [*cog-1^{prom}::GFP; dpy-20 (+)*]; and ASEL/R markers *otIs151*V=Is[*ceh-36^{prom}::DsRed2; rol-6(d)*], *otIs125*=Is[*flp-6^{prom}::GFP*], *oyIs59*=Is[*osm-6::GFP; lin-15 (+)*], *otIs188*=Is[*che-1::YFP; rol-6(d)*] and *otIs217*=Is*[che-1^{prom}::HIS-3::mCherry; rol-6(d)]*. Reporters for other cell types included: *pkIs531*=Is[*gpa-9::GFP; lin-15 (+)*], *ynIs2022*III=Is[*flp-8^{prom}::GFP; rol-6(d)*], *oyIs17*=Is[*gcy-8^{prom}::GFP; lin-15 (+)*], *kyIs104*X=Is[*str-1::GFP; lin-15 (+)*], *kyIs140*=Is[*str-2::GFP; rol-6(d)*], *gmIs12*=Is[*srb-6::GFP; rol-6(d)*], *otIs182*=Is[*inx-18^{prom}::GFP*], *oyIs14*V=Is[*sra-6::GFP; lin-15 (+)*], *mgIs18*=Is[*ttx-3::GFP; lin-15 (+)*], *otIs138*=Is[*ser-2^{prom}::GFP; rol-6(d)*], *vtIs1*=Is[*dat-1::GFP; rol-6(d)*], *bgIs312*I=Is[*pes-6::GFP*], *mgIs20*=Is[*lim-6::GFP; rol-6(d)*], *oxIs12*X=Is[*unc-47^{prom}::GFP; lin-15 (+)*] and *otIs173*=Is[*F25B3.3::DsRed2; ttx-3::GFP*]. Other transgenic lines: *otEx3362*=Ex[*nhr-67::mCherry*; *elt-2::GFP*], *otEx3910*=Ex*[cog-1promAnhr-67sitedel::gfp; elt-2::gfp]* and *otEx3761*=Ex*[cog-1promA::gfp; elt-2::gfp]*.

lsy-9/*nhr-67* alleles

In several previously described genetic screens, we identified four alleles of *lsy-9*, *ot85*, *ot136*, *ot202* and *ot210*, which display a heterogeneous class V Lsy phenotype (Sarin et al., 2007). We have since found that three other mutant alleles, *ot158*, *ot190* and *ot247*, previously considered separate genetic loci (Sarin et al., 2007) are in fact allelic to *lsy-9*. *ot158* was considered a separate genetic locus owing to its distinct phenotype (class I '2 ASEL' phenotype). Mapping of *ot158* revealed it to be linked to the *lsy-9* locus, and allele sequencing, transformation rescue and complementation tests determined that *ot158* is an allele of *lsy-9*. *ot190* was initially mapped onto a separate chromosome (Sarin et al., 2007), yet further analysis revealed that the SNP marker used for this analysis, F32B5, provided misleading mapping data. *ot190* was found to be allelic to *lsy-9* by allele sequencing and complementation tests. *ot247* was placed into a distinct complementation group from *lsy-9* owing to its failure to complement another *lsy* gene, *lsy-18*. However, allele sequencing, additional complementation tests and rescue analysis showed that *ot247* is an allele of *nhr-67*. The genome knockout consortia generated three separate deletion alleles of *lsy-9* that are very similar in molecular nature and we therefore only analyzed one of them, *ok631*. One additional *lsy-9/nhr-67* allele, *ot407*, was retrieved by a non-complementation screen. For this screen, a balanced strain with the genotype *nhr-67(ok631)/mgIs18 unc-24; Ex[nhr-67-fosmid; elt-2::gfp]* was generated. Heterozygous animals are viable, non-Unc, express *gfp* in the AIY interneuron (*mgIs18*/+), and express, with limited penetrance, *elt-2::gfp* in the intestine, which marks a rescuing array with the *nhr-67*-containing fosmid. Progeny of this balanced strain will be of the same genotype, will be of the genotype *mgIs18 unc-24/mgIs18 unc-24* (and therefore Unc) or will be *ok631/ok631*, and all viable adults will display green intestinal cells as they need the array to rescue the *ok631* lethality. We mutagenized several populations of this strain using EMS as previously described (Brenner, 1974; Gengyo-Ando and Mitani, 2000). We selected for animals in the next generation that are heterozygous, i.e. non-Unc, and displayed expression of *gfp* in AIY (from *mgIs18*), but nevertheless contain the *elt-2::gfp* marked rescuing array with complete penetrance. Such animals are supposedly of the *nhr-67(ok631)/mgIs18 nhr-67(new allele) unc-24* genotype, as they require the rescuing array to live to adulthood. We then homozygosed *nhr-67(new allele)* by selecting for Unc animals in the next generation and subsequently sequenced the *nhr-67* locus in inviable, non-transgenic progeny. We retrieved one allele from this screen, *ot407*.

Reporter genes

che-1 and *nhr-67* reporter genes were created using λ-Red-mediated recombineering in bacteria as described (Dolphin and Hope, 2006; Tursun et al., 2009). Briefly, the *che-1*-containing fosmid (WRM066bC03) and the *nhr-67*-containing fosmid (WRM0613bE08) were each electroporated and maintained in the *E. coli* strain EPI-300 T1R (Epicentre). Using tetA recombineering cassettes for two-step counter selection with tetracycline and streptomycin, or using the more efficient *flp* recombinase-removable *galK*-based cassettes, we inserted *yfp* (*che-1*) or *mCherry (nhr-67*, *che-1*) immediately preceding the stop codon at the C terminus of the respective gene, which resulted in a translational fusion at each locus. Recombineered fosmids were sequenced at their recombineered junctions. For the *che-1::yfp* and *che-1::mCherry* fosmid injection, the fosmid was digested with *Sac*II and injected at 10 ng/μl, together with *Sca*I-digested *rol-6(d)* (pRF4; 2 ng/ul) and *Pvu*II-digested N2 genomic DNA (100 ng/μl) to generate a complex array. The DNA was injected into *che-1(ot94)*; *ntIs1*. After integration of the *che-1::yfp* fosmid array by gamma irradiation *ntIs1* was outcrossed during backcrossing. The resulting array is called *otIs188*. For the *nhr-67::mCherry* fosmid injection, the fosmid was injected at 50 ng/μl, together with 30 ng/μl *elt-2::gfp* (pJM67) and 50 ng/μl pBluescript carrier DNA. The DNA was injected into *nhr-67(ok631)/nT1*. The resulting array is called *otEx3362*.

Expression analysis of *nhr-67*

The *nhr-67::mCherry* fusion DNA was co-injected (50 ng/μl) with *elt-2::GFP* (30 ng/μl) into balanced *ok631*/nT1 animals to ascertain rescuing ability. Cells expressing *nhr-67* were identified using 4D microscopy and SIMI BioCell software as described (Schnabel et al., 1997). Briefly, *otEx3362* (*nhr-67::mCherry; elt-2::GFP*) gravid adults were dissected and single two-cell embryos were mounted and visualized on a Zeiss Axioplan 2 compound microscope. Nomarski stacks were taken every 35 seconds and images within a stack at ~1 μm apart. Embryos were flashed with TRIT-C-filtered fluorescence at pre-determined time points corresponding to periods between divisions within the AB lineage. After a fluorescent flash, the movie was suspended and embryos were scored for presence of *elt-2::GFP* (and therefore the array). Movies of embryos not containing the array were discarded. At least two movies were taken per AB^x cell stage, i.e. AB^4 cells, AB^8 cells, AB^{16} cells, etc., until the bean stage. Movies were lineaged using the SIMI BioCell program. Two *nhr-67*-expressing blastomeres at the mid-gastrulation stage could not be identified owing to technical limitations. Larval and adult *nhr-67* expression was determined by nuclei position and cell body morphology of *mCherry*-expressing cells. The transgene *osm-6::gfp* (*oyIs59*) was also used in the background to help establish the relative positions of these cells. One pair of neurons just posterior to the RIR neuron showed dim expression and were likely to be the RICL/R neurons, but could

not be reliably identified owing to their variable positioning. Three cells anterior to the anterior ring ganglia were not identified but were likely to be socket and/or pharyngeal neurons.

Yeast one-hybrid analysis

Yeast one-hybrid experiments were conducted as described previously (Deplancke et al., 2004). A 1.8-kb fragment including the conserved NR2E motif and ASE motifs was amplified from two constructs, cog-1promA (O'Meara et al., 2009) and cog-1promA nhr-67 del., in which the conserved sequence AAGTCA had been deleted. The resulting constructs were named cog-1promD and cog-1promD nhr-67site del. Each construct was cloned by the Gateway recombination system into pMW2 (Addgene), which contains the His3 reporter. Each vector was subsequently linearized with *Xho*I and integrated into the Y1H strain YM4271 at the *his3-200* locus. Integrants were selected on Sc-His media. Transformations and integrations were performed as described (Deplancke et al., 2004). One hundred nanograms of AD-NHR-67 Destination clone DNA and empty vector DNA (OpenBiosystems) were transformed into each DNAbait:reporter strain. Transformations were plated on SC-Trp media. Thirty-two transformants were randomly selected from each transformation and diluted in 100 μl of water. Four microliters of each dilution were plated on SC –Trp, SC –Trp –His, and SC –Trp –His + 40 mM 3-AT plates. Plates were incubated for 5 days at 30°C and then scored.

RESULTS

lsy-9 mutants display a complex phenotype in the development of left/right asymmetric ASE neurons

lsy-9(ot85) mutant animals were retrieved in a screen for mutants in which the L/R asymmetric fate of the ASE neurons fails to be appropriately executed (Sarin et al., 2007). *lsy-9* mutants display a disruption of L/R asymmetric gene expression profiles in ASEL/R, as has previously been shown with a single allele, *ot85*, using the ASEL fate marker *lim-6::gfp* and the ASER fate marker *gcy-5::gfp* (Sarin et al., 2007) (Table 1, Fig. 2A). We have broadened this analysis to include several more alleles of *lsy-9*, some newly isolated and not

Table 1. ASE fate in *lsy-9/nhr-67* mutant animals

			Percentage of animals with *gfp* expression in ASEL/R*						
	Fate marker	Genotype	●○	●○	●●	○○	○●	○●	*n*
ASEL markers	*gcy-7 (otIs3)*	Wild type	100	0	0	0	0	0	>100
		ot85	45.3	0	16.3	23.3	0	15.1	86
		ok631	32.8	0	24.6	28.7	0	11.5	80
	lim-6 (otIs114)	Wild type	100	0	0	0	0	0	>100
		ot85	54.8	1.2	13.1	23.8	0	7.1	84
		ok631	32	0	28	30	0	10	50
		ot136	80	0	10	8	0	2	50
		ot202	41.4	5.2	24.1	17.2	0	12.1	58
		ot210	79.2	1.9	3.8	11.3	0	3.8	53
		ot158	77.5	0	21	1.5	0	0	137
		ot190	66.7	0	12.3	17.5	0	3.5	57
	lsy-6 (otIs160)	Wild type	91.4	0	0	8.6	0	0	35
		ot85	62.5	16.7	2.1	14.6	0	4.2	48
ASER markers	*gcy-5 (ntIs1)*	Wild type	0	0	0	0	0	100	>100
		ot85	0	0	0	33	0	67	97
		ok631	0	0	0	61.2	1.2	37.6	82
		ot407	0	0	0	69	0	31	51
		ot158	0	0	0	16	0	84	50
	cog-1 (syIs73)	Wild type	0	0	0	3	24.6	72.4	29
		ot85	0	0	0	51.4	0	48.6	37
					●●	○○	●○ or ○●		
ASEL/R bilateral markers	*ceh-36 (otIs151)*	Wild type			100	0	0		>100
		ok631			44	24	31		86
		ot85			59	9	32		98
		ot158			100	0	0		25
	che-1 (otIs188)	Wild type			100	0	0		>100
		ok631			28	35	37		51
		ot158			100	0	0		40
	flp-6 (otIs125)	Wild type			100	0	0		20
		ok631			53.7	9.3	37.0		54
		ot85			72	10	17		98
	osm-6 (oyIs59)	Wild type			100	0	0		>100
		ok631			71.4	0	29.6		27

*Circles indicate *gfp* expression levels in the pair of left and right ASE neurons.

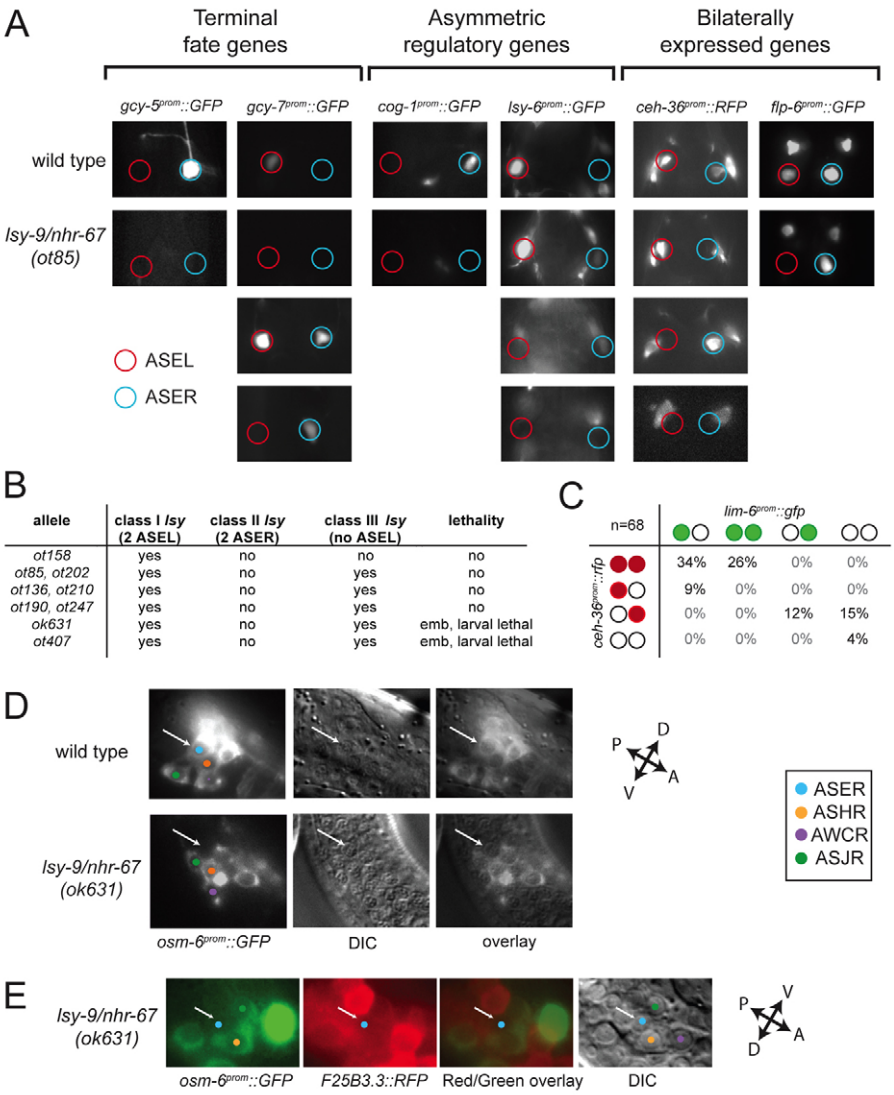

Fig. 2. Defects observed in *lsy-9/nhr-67* mutant animals. (**A**) *lsy-9/nhr-67* regulates ASEL-, ASER-specific and bilateral cell fate markers. Quantification of these data can be found in Table 1. Strains presented from the second row down contain *lsy-9(ot85)* in the background. Animals were scored as adults. (**B**) Allelic series of *lsy-9* alleles. (**C**) Apparent L/R reversal defects are caused by a mixture of class I ('2 ASEL') and class III ('no ASE') mutant phenotypes, as revealed by a correlation analysis in which *lim-6* (ASEL fate) and *ceh-36* (ASEL+ASER bilateral fate) are simultaneously scored with reporter transgenes (*lim-6::gfp–otIs114; ceh-36::rfp–otIs151*) in a *lsy-9(ot85)* mutant background. (**D**) *lsy-9/nhr-67* positively regulates expression of the ciliated sensory marker *osm-6*, as scored with *osm-6::gfp* (*oyIs59*). White arrow indicates presence or absence of *osm-6* expression in ASE, which was identified by its location relative to surrounding amphid sensory cells. Nomarski image indicates that the ASE nucleus is still present, immediately posterior to ASH. (**E**) *lsy-9/nhr-67* does not affect expression of the pan-neuronal marker *F25B3.3*. Colored dots indicate cell types as in D. D, dorsal; V, ventral; A, anterior; P, posterior.

described before (Table 1; see also Materials and methods). All alleles are recessive. Four of the six available *lsy-9* alleles are homozygous viable, two of them display an early larval arrest phenotype (phenotypic categories of all alleles are summarized in Fig. 2B). With the exception of *ot158*, discussed in more detail below, all alleles display a similar wide range of phenotypes: in larval and adult animals, the ASEL fate marker *lim-6::gfp* is either unaffected, bilaterally expressed in both ASEL and ASER, expressed in neither ASEL nor ASER, or expressed exclusively in ASER (Table 1). We used a subset of the available alleles to analyze an additional panel of reporters. We found that the ASEL marker *gcy-7* shows a similar range of phenotypes as the *lim-6* fate marker (Fig. 2A, Table 1). Moreover, expression of the miRNA *lsy-6*, an essential trigger of ASEL fate, which is normally only expressed in ASEL, is de-repressed in ASER and/or is lost in ASEL (Fig. 2A, Table 1).

In contrast to the variety of phenotypes observed with ASEL markers, ASER markers show only one phenotype: ASER marker expression (the terminal differentiation marker *gcy-5* or the ASER inducer *cog-1*) is either normal or lost (Fig. 2A, Table 1). ASER marker expression does not therefore present the mirror image of ASEL marker expression, i.e. in those cases in which ASEL marker expression is lost, there is no concomitant gain of ASER marker expression.

The analysis of bilaterally expressed markers, the homeobox gene *ceh-36* and the FMRFamide gene *flp-6*, displayed an unexpected phenotype. Expression of the bilateral markers was unaffected, lost in either ASEL or ASER, or lost in both (Fig. 2A, Table 1). This observation raised the possibility that the loss of asymmetric fate markers, such as *lim-6::gfp*, might not be a reflection of a laterality defect in which left fate has converted to the right fate, but might rather be reflective of an overall differentiation defect of ASE. To assess this possibility, we analyzed ASEL fate and bilateral fate simultaneously, using *rfp*-tagged *ceh-36* (bilateral marker) and *gfp*-tagged *lim-6* (ASEL marker). We found a perfect correlation of loss of ASEL fate and loss of the bilateral fate marker (Fig. 2C). Moreover, whenever ASE fate was executed in either ASEL or ASER, as assessed by normal *ceh-36* expression, the neuron was likely to express the ASEL fate marker *lim-6* (Fig. 2C). This observation provides an explanation for what appears to be a 'reversal defect' in which ASEL fate is only expressed in ASER. In those animals, the left neuron does not differentiate (no *ceh-36* expression), but the right neuron differentiates and aberrantly executes the left fate. In conclusion, the *lsy-9* phenotype is a mixture of what we previously termed a class III phenotype ('no correct bilateral ASE fate specification') and a class I phenotype ('2 ASEL', instead of '1 ASEL+ 1 ASER') (Sarin et al., 2007).

lsy-9 acts both upstream and downstream of *che-1*

The failure of ASE to express asymmetric and bilateral markers could reflect an inability to differentiate or could indicate a fate transformation in which ASEL or ASER have adopted the fate of their respective sister cell, which normally undergoes programmed cell death (see Fig. S1 in the supplementary material). To test this possibility, we generated a *lsy-9; ced-4* double mutant in which cell death is inhibited. In those animals, the loss of marker gene expression is not alleviated. Instead, ectopic ASE marker expression is occasionally observed in the now undead sisters of ASEL and ASER (see Fig. S1 in the supplementary material).

The other possibility for a loss of ASE fate marker expression is that *lsy-9* acts upstream of the ASE fate inducer *che-1*, which encodes a C2H2 zinc-finger transcription factor (Chang et al., 2003; Etchberger et al., 2007; Uchida et al., 2003). A loss of *che-1* would be expected to lead to a loss of expression of both bilateral and asymmetric features of ASE (class III phenotype) (Chang et al., 2003; Etchberger et al., 2007; Uchida et al., 2003). We tested this possibility by examining *che-1* expression in *lsy-9* mutants, using a fosmid-recombineered *che-1* reporter construct (Tursun et al., 2009). This construct, *che-1::yfp*, contains the entire *che-1* locus together with three upstream and two downstream genes, is engineered to contain *yfp* fused to the last exon of *che-1* and rescues the *che-1* mutant phenotype. Postembryonically, this reporter is exclusively expressed in ASEL and ASER throughout larval and adult stages. In the embryo, expression is also exclusively observed in a pair of cells, starting at the ABalpppppppa/ABpraaapppa stage (Fig. 3A). These two cells are the mothers of the two ASE neurons. Expression persists throughout cell division of the ASE mother, which produces ASE(L/R) and a cell that undergoes programmed cell death. Similar expression was observed with a *che-1::mCherry* construct (data not shown). In *lsy-9* mutants, *che-1* expression is lost in a large fraction of animals (Fig. 3A; see also Fig. S2 in the supplementary material), suggesting that *lsy-9* positively regulates *che-1*, which then induces general ASE fate. By contrast, *lsy-9* expression is not affected in *che-1* mutants (see below). It is formally possible that after *che-1* induction, *lsy-9* and *che-1* might cooperate to induce ASE fate, but this appears unlikely as ectopic, *gpa-10* promoter-driven expression of *che-1* in cells that do not normally express *lsy-9* (as described below) is sufficient to induce the expression of ASE-specific terminal differentiation markers (Uchida et al., 2003). Moreover, *lsy-9* expression is not maintained in ASE (as described below), whereas *che-1* expression is, and this maintained *che-1* expression is crucial to maintain ASE fate (Etchberger et al., 2009). *che-1* therefore does not appear to need *lsy-9* to control bilateral ASE fate.

The role of *lsy-9* is not restricted to controlling *che-1* expression, as *lsy-9* defects are more severe than *che-1* null mutant effects. In a fraction of *lsy-9* animals, the ASE dendrites do not develop appropriately; they are either too short or they overextend (Fig. 3B).

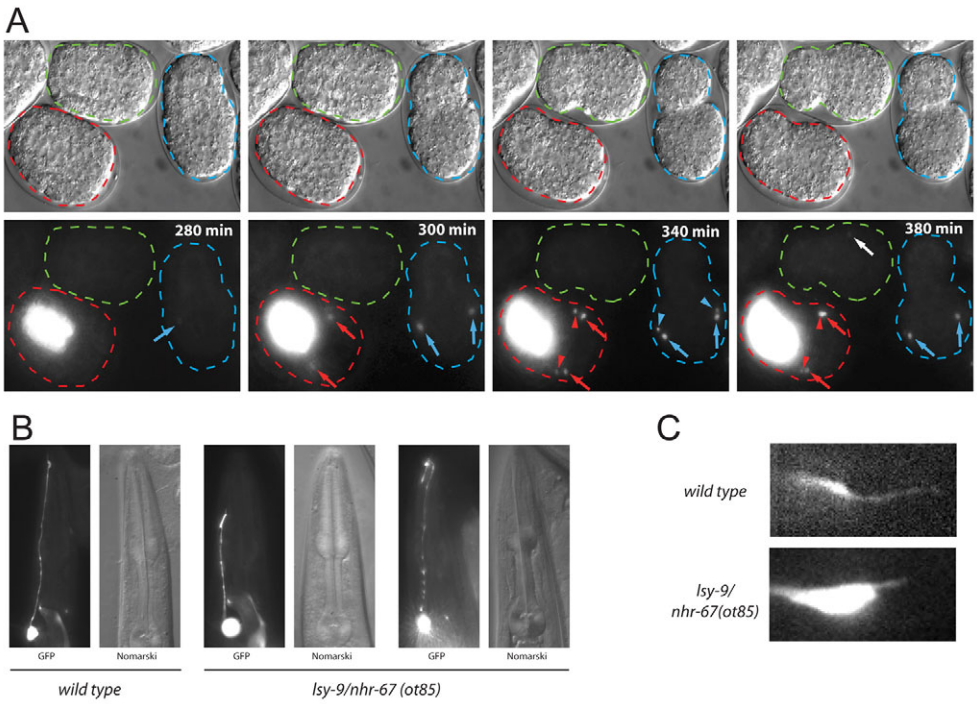

Fig. 3. *lsy-9/nhr-67* acts upstream of *che-1*. (**A**) Embryonic *che-1* expression. Nomarski images (top row); fluorescence (bottom row). Three genotypically distinct embryos are highlighted at sequential time points postfertilization at 20°C, from the onset of *che-1* expression (~280 minutes) to almost complete engulfment of the dead sister cell of ASE (~380 minutes). *che-1::yfp (otIs188)* expression is shown in a wild-type embryo (blue), in an *lsy-9/nhr-67(ok631)* mutant embryo (green) and in an *lsy-9/nhr-67(ok631)* mutant embryo rescued by a *nhr-67(+)* array [*otEx3103=Ex(nhr-67fosmid; elt-2::gfp)*, red]; note that the strong *gfp* signal is the *elt-2::gfp* injection marker. Arrows indicate ASE expression of *che-1::yfp*; arrowheads indicate the ASE sister cell, which eventually undergoes apoptosis and is consumed by the ASE cell. For quantification, see Fig. S1 in the supplementary material. (**B**) *lsy-9/nhr-67* mutants display ASE dendrite defects. Fluorescent and Nomarski images of ASEL dendrites of wild-type and *lsy-9/nhr-67* mutant adult hermaphrodites are shown. Dendrites were visualized using the ASEL-specific transgene *lim-6^{prom}::gfp* (=*otIs114*). The penetrance of defects is 16% (*n*=50) in *lsy-9/nhr-67(ot85)* and 7% (*n*=55) in *lsy-9/nhr-67(ok631).* (**C**) Cilia defects of ASE neurons in adult *lsy-9/nhr-67* mutants. The ASE sensory ending (a thin line immediately following the thicker projection) was visualized using the ASEL-specific transgene *lim-6^{prom}::gfp* (=*otIs114*). The cilium is full length in wild-type animals but stubby and bloated in *lsy-9/nhr-67* mutant animals. Defects were observed in 9% (*n*=44) of *nhr-67(ot85)* animals.

In those cases in which the dendrites appear to be appropriately established, the ciliated ultrastructure is defective (Fig. 3C). Moreover, expression of the cilia marker *osm-6* is lost in *lsy-9* mutants (Fig. 2D). These defects extend beyond those of *che-1* mutants, which express *osm-6* normally and have normally extended dendrites and ciliated endings (Lewis and Hodgkin, 1977; Uchida et al., 2003) (data not shown). In *che-1* mutants, ASE is able to take up the dye DiI through exposed sensory endings (Uchida et al., 2003); this ability is abrogated in *lsy-9* mutants (data not shown). In both *lsy-9* and *che-1* mutants, pan-neuronal fate is executed normally (Uchida et al., 2003) (Fig. 2E). These findings suggest that *lsy-9* and *che-1* progressively define the identity of ASE. *lsy-9* controls broad aspects of ASE fate, including the ciliated sensory neuron identity of ASE, whereas *che-1* defines the type of ciliated sensory neuron.

As noted above, the fraction of *lsy-9* animals that expresses *che-1* and bilateral terminal ASE features will execute the 'ASEL fate' on both sides of the animal (class I phenotype), indicating that *lsy-9* has a separate role in inducing ASER fate. The *ot158* allele appears to genetically separate these two functions, as *ot158* mutants execute bilateral ASE fate normally (normal *che-1* and *ceh-36* expression), but these animals display the class I phenotype (ASER to ASEL switch) that is reflective of a participation in the bistable feedback loop that controls ASEL versus ASER fate (Table 1).

We considered the possibility that the asymmetry defects observed in *lsy-9* mutants are a mere reflection of reduced *che-1* activity. Several lines of evidence indicate that this possibility is unlikely. First, we raised the levels of *che-1* activity in *lsy-9(ot158)* mutants (in which bilateral fate is executed properly, but asymmetry of fate is not), using a transgene that expresses *che-1* under the control of a heterologous promoter (*ceh-36prom::che-1*), and found that this did not rescue the *lsy-9* defects (data not shown). Second, we have recently identified a hypomorphic, partial loss-of-function allele of *che-1* that results in the opposite defect to the one we observe in *lsy-9* animals – a '2 ASER' phenotype, rather than the *lsy-9*-type '2 ASEL' phenotype (Etchberger et al., 2009). *nhr-67* therefore appears to have separable functions in first inducing ASE fate and then controlling ASEL/R asymmetry.

To assess in more detail how *lsy-9* fits into the previously described bistable feedback loop that controls ASEL versus ASER fate, we generated double mutants of *lsy-9* with several mutants in components of the bistable feedback loop controlling ASEL/R asymmetry (shown in Fig. 1). We found that the completely penetrant loss of ASEL fate in animals lacking the miRNA *lsy-6* was suppressed in *lsy-9* mutants (Table 2). Moreover, the ASER neuron still ectopically executed ASEL fate in *lsy-9* mutants in the absence of *lsy-6* (Table 2). These epistasis data suggest that the asymmetry-determining role of *lsy-9* lies, at least in part, downstream of *lsy-6*. Ectopic expression of the ASER fate inducer *cog-1* in ASEL, observed in the gain-of-function allele *cog-1(ot123)*, a 3′UTR deletion, results in a partially penetrant conversion of ASEL to ASER fate (Sarin et al., 2007). This effect was suppressed by *lsy-9(ot85)*, indicating that *lsy-9* is required for *cog-1* function (Table 2). The completely penetrant loss of ASEL fate in animals defective in *die-1*, the output regulator of the bistable feedback loop (Fig. 1), was not suppressed by *lsy-9* (Table 2), indicating that *lsy-9* may act upstream of *die-1*. In summary, this genetic analysis places *lsy-9* into the bistable regulatory loop, at a position downstream of the miRNA *lsy-6*, but upstream of the output regulator *die-1*.

lsy-9 affects the identity of many distinct neuron types

We also investigated whether the effect of *lsy-9* is restricted to the ASE neurons or extends to lineally related cells. We examined neuron-type-specific fate markers for a number of different neuronal lineages that emanate from the ABalppp neuroblast, which generates ASEL and 11 other neurons, plus two glial-like cells (Fig. 4A). We found that the expression of fate markers for the neurons closely related to ASE (sister, cousins) was affected (Fig. 4A,B; see Table S1 in the supplementary material). A subset of more distally related neurons was also affected, whereas several other neuron classes were not (Fig. 4A,C; see Table S1 in the supplementary material). We extended this fate marker analysis to a variety of distinct neuron classes throughout the AB lineage (which generate >90% of the *C. elegans* nervous system) and found that *lsy-9* affects the development of 13 out of the 22 neuron classes tested (see Table S1 in the supplementary material). There appears to be no common theme in the type of neurons affected. Defects were observed in sensory, inter- and motoneurons (Fig. 4C). Affected neurons do not fall into a specific neurotransmitter class and affected neurons do not derive from a single common lineage branch. However, many of the cells affected were sister or cousin cells (Figs 4, 6), which suggests

Table 2. Genetic interaction tests

	ASEL		ASER	
Genotype	% animals with *lim-6::gfp**	% animals with *gcy-5::gfp*†	% animals with *lim-6::gfp*	% animals with *gcy-5::gfp*
Wild type	100 (*n*>100)	0 (*n*>100)	0 (*n*>100)	100 (*n*>100)
lsy-9(ot85)‡	100 (*n*=68)	0 (*n*=97)	44 (*n*=68)	67 (*n*=97)
lsy-9(ok631)§	100 (*n*=50)	0 (*n*=82)	64 (*n*=50)	36 (*n*=82)
lsy-6(ot71)	0 (*n*=25)	100 (*n*=43)	0 (*n*=25)	100 (*n*=43)
lsy-6(ot71); lsy-9(ot85)‡	22 (*n*=52)	nd	21 (*n*=52)	nd
lsy-6(ot71); lsy-9(ok631)§	67 (*n*=60)	43 (*n*=61)	67 (*n*=60)	55 (*n*=61)
die-1(ot26)	0 (*n*=50)	100 (*n*=50)	0 (*n*=50)	100 (*n*=50)
die-1(ot26); lsy-9(ot85)‡	0 (*n*=34)	nd	0 (*n*=34)	nd
die-1(ot26); lsy-9(ok631)§	nd	100 (*n*=30)	nd	100 (*n*=30)
cog-1(ot123)	nd	100 (*n*=50)	nd	100 (*n*=50)
cog-1(ot123); lsy-9(ok631)§	nd	56 (*n*=105)	nd	74 (*n*=105)

*Transgene used was *otIs114 (lim-6^{prom}::gfp)*.
†Transgene used was *ntIs1 (gcy-5^{prom}::gfp)*.
‡*ceh-36::rfp (otIs151)* is in the background and only those animals that showed normal *ceh-36::rfp* expression were scored. Animals showed consistent numbers for L1 and adult scoring. L1 numbers are presented.
§*che-1::mCherry* (*otIs217*) is in the background and only those animals that showed normal *che-1::mCherry* expression were scored. These animals were scored as L1s due to lethality of *ok631*.
nd, not determined.

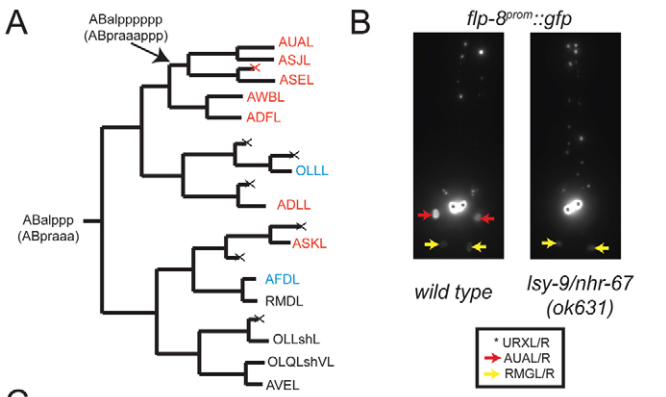

C

	Fate affected in *lsy-9/nhr-67*	Fate not affected in *lsy-9/nhr-67*
Sensory neurons	ASE, ASJ, AWB, ASK, ADL, ADF, ASH, AWC, dopamine neurons [1]	AFD, ASI, OLL, ADE, CEP
Interneurons	AUA, AVG, RIS	AIY, PVQ
Motorneurons	RME, AVL	D-type MNs

Fig. 4. *lsy-9/nhr-67* broadly affects neuronal fate. (**A**) Lineage diagram of the ABalppp neuroblast. Neurons whose fate was affected in *lsy-9/nhr-67* mutants are indicated in red, those unaffected are in blue, and those untested are in black. See Materials and methods for fate markers used. (**B**) Representative image of a fate marker lost in *lsy-9/nhr-67* mutants. The transgene used to visualize AUA is *flp-8*^{prom}*::gfp* (=*ynIs2022*). *ynIs2022* is normally expressed in three cell types: URX, AUA and RMG. *nhr-67* mutants specifically affect *flp-8* expression in AUA (L/R; red arrows). For quantification, see Table S1 in the supplementary material. (**C**) Summary of all neuronal fates tested in *lsy-9/nhr-67* mutant background. [1]The dopamine neuron marker was expressed ectopically in unidentified cells. For markers and alleles used and penetrance of defects, see Table S1 in the supplementary material.

that *lsy-9* might affect the identity of the neuroblasts that generate them. This notion conforms to the expression pattern of *lsy-9*, as described further below.

lsy-9 is allelic to the Tailless-related orphan nuclear receptor *nhr-67*

We mapped *ot85* to a small chromosomal interval on linkage group 4. Transformation rescue experiments revealed rescue of *lsy-9* mutants with a single fosmid containing 11 predicted genes (Fig. 5). One gene on the fosmid is the orphan nuclear hormone receptor *nhr-67*, first identified by a genome-wide sequence analysis of nuclear hormone receptor genes (Sluder et al., 1999). Sequencing all available *lsy-9* alleles, we found mutations in the coding region of *nhr-67* in all mutant strains (Fig. 5). Moreover, a deletion allele generated by the Oklahoma *C. elegans* knockout consortium (kindly provided by R. Barstead), as well as RNAi directed against *nhr-67*, recapitulated the *lsy-9* mutant phenotype (Table 1; data not shown). We conclude that *lsy-9* is *nhr-67*, and from here on refer to this gene as *nhr-67*.

Reciprocal BLAST searches, phylogenetic analysis and specific sequence features show that NHR-67 is an ortholog of the fly Tailless and the vertebrate TLX transcription factors (Fernandes and Sternberg, 2007; Sluder et al., 1999). Several mutant alleles, the first yet described for *nhr-67*, illustrate the importance of individual domains of NHR-67 (Fig. 5). Besides a mutation in a Zn-coordinating Cys residue in the DNA-binding C4-type zinc-finger domain, one allele, *ot190*, contains a missense mutation that affects a residue in the P-box, a crucial component of DNA-binding specificity (Yu et al., 1994). Another missense mutation, *ot158*, affects the so-called AF2 motif, which is involved in transcriptional activation in other nuclear hormone receptors (Durand et al., 1994) (Fig. 5). It was this mutation that resulted specifically in a loss of ASEL/ASER asymmetry (class I '2 ASEL' phenotype), without affecting the bilateral specification of ASE (Table 1).

The deletion allele provided by the knockout consortium, *ok631*, results in an out-of-frame deletion of C-terminal exons and might destabilize the whole message. This allele is similar in severity to the other five class V alleles, i.e. it produces a mixed class I ('2 ASEL neurons') and class III ('no ASE neuron') phenotype. In contrast to other alleles, however, *ok631* animals are inviable, with death occurring at a range of different stages from post-gastrulation embryos to the first larval (L1) stage. This pleiotropy could be rescued by the *nhr-67*-containing fosmid (data not shown). Postembryonic death is likely to be caused, at least in part, by dysfunction of the excretory system, as at least one cell of the excretory system, the excretory canal cell, displayed cystic phenotypes (see Fig. S3 in the supplementary material), which is reminiscent of other excretory canal cell mutants (Buechner et al., 1999).

None of the initially identified *nhr-67* alleles (*ot85*, *ot136*, *ot158*, *ot190*, *ot202*, *ot210*), nor the deletion allele, is a definitive molecular null allele. The ASE phenotype of the canonical *ot85* allele was not enhanced by RNAi against *nhr-67* (using a sensitized *nre-1 lin-15b; nhr-67(ot85)* strain) or by placing *ot85* over a deficiency (data not shown), which is consistent with *ot85* being a very strong loss-of-function allele. To further explore the null allele issue, we also undertook a non-complementation screen for additional *nhr-67* alleles (see Materials and methods), isolating a mutant allele, *ot407*, in one of the Zn co-ordinating Cys residues of the C4 zinc-finger domain. Like *ok631*, *ot407* animals arrest as embryos or L1, yet their ASE phenotype is no more severe than that of other available strong loss-of-function mutants.

Expression pattern of *nhr-67*

How does the expression pattern of *nhr-67* fit with the multiple roles of *nhr-67* in ASE development? Previously described *nhr-67* reporter genes did not incorporate the full *nhr-67* locus and therefore provided no rescuing gene activity (Fernandes and Sternberg, 2007; Gissendanner et al., 2004). We engineered the *mCherry* coding region into the last exon of *nhr-67* within the context of a ~40-kb fosmid that contains the *nhr-67* locus and 5 genes upstream and downstream of the *nhr-67* fosmid using bacterial recombineering. The resulting *nhr-67::mCherry* reporter rescues both the ASE phenotype and larval arrest phenotype of *nhr-67(ok631)* mutants (7 out of 9 transgenic lines).

Within the ASEL/R generating lineages, *nhr-67::mCherry* was first observed in the grandmother cells of ASEL and ASER. Those grandmother cells divide twice more to yield the respective ASE neuron and a sibling cell that undergoes programmed cell death (Sulston et al., 1983) (Fig. 6A). To compare *nhr-67::mCherry* expression with the onset of *che-1* expression, we used the *che-1::yfp* fosmid described above. Transgenic animals that co-express a functional *nhr-67::mCherry* reporter and a functional *che-1::yfp* reporter revealed that *nhr-67* precedes *che-1* expression (Fig. 6B). Consistent with a role of *nhr-67* upstream of *che-1*, we found that *nhr-67* expression is unaffected in *che-1* mutants (data not shown). *nhr-67* expression was maintained in the ASEL and ASER neurons until the first larval stage after which it became undetectable, whereas *che-1* expression was maintained throughout the life of the

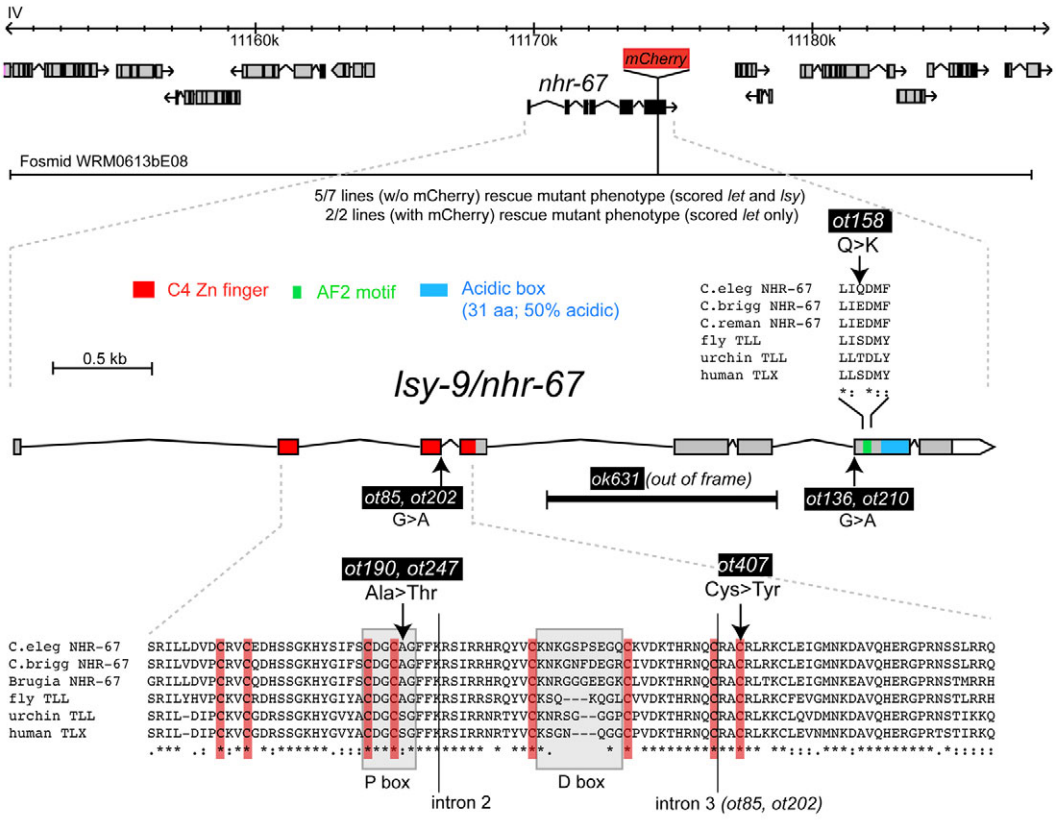

Fig. 5. Cloning of *lsy-9/nhr-67*. The chromosomal location of *lsy-9/nhr-67*, the fosmid used for transformation rescue and expression pattern analysis, and the location of individual mutant alleles are indicated. An *nhr-67::mCherry* fusion was created using recombineering into the rescuing fosmid. Alleles with the same molecular identity were independently isolated.

animal. In spite of its genetically deduced role in asymmetric gene expression in ASEL and ASER, *nhr-67* expression is bilaterally symmetric in ASEL and ASER.

Apart from cells in the neuroblast lineage that generate ASE, *nhr-67::mCherry* was expressed in multiple other neuroblast lineages in the developing embryo. Expression was usually observed in the grandmother or mother of a neuron, but not earlier (Fig. 6A). Within the ASEL and ASER-generating lineage branches, *nhr-67* was expressed in neuroblasts that generate closely or distantly related cousins of ASEL and ASER and this expression was highly consistent with defects observed in those lineages. For example, the sister neuroblast of the ASE-generating neuroblast creates the AUA and ASJ neurons and it expressed *nhr-67* (Fig. 6). Both AUA and ASJ failed to undergo the normal differentiation program in *nhr-67* mutants (Fig. 4; see Table S1 in the supplementary material). The cousin of the ASE-mother cell generates the AWB and ADF sensory neurons. *nhr-67* was expressed in these cells and its loss resulted in differentiation defects, as assessed by examining the serotonergic fate of ADF and chemoreceptor expression in AWB. These differentiation defects could be explained by *nhr-67* regulating expression of the LIM homeobox gene *lim-4* (see Table S1 in the supplementary material), a regulator of ADF and AWB cell fate (Sagasti et al., 1999; Zheng et al., 2005). However, *nhr-67* function extends beyond regulating *lim-4*, because the partially penetrant loss of ADF fate, as measured by *tph-1* expression, in *lim-4* null mutants was enhanced by *nhr-67* (see Table S1 in the supplementary material).

In late stage embryos, a few other, postmitotic neurons started to express *nhr-67* (Fig. 6C). Embryonic *nhr-67* expression was not restricted to the nervous system, but was observed in a small subset of mesodermal and hypodermal cells (Fig. 6A). No expression was detected in endodermal cells or the germ line. Consistent with its excretory canal cell mutant phenotype (see Fig. S3 in the supplementary material), *nhr-67* was expressed in the excretory canal cell.

Postembryonically, *nhr-67* expression persisted only in a few neurons in the head ganglia until the first larval stage and faded shortly thereafter in most, but not all, of these neurons, with expression persisting through adulthood only in the CEPD/V, RMED/V, AVL and RIS neurons (Fig. 6C). During mid-larval development, *nhr-67* was transiently and dynamically expressed in the AC cells of the vulva, as previously described (Fernandes and Sternberg, 2007). Expression was also found in the VU cells and somatic gonad, but not in vulA, vulB or vulC, as has been previously shown with smaller reporter constructs that might not contain all of the relevant *cis*-regulatory information (Fernandes and Sternberg, 2007).

The cellular expression profile of *nhr-67* largely overlapped with the profile of cellular defects (Fig. 4C, Fig. 6A; see also Table S1 in the supplementary material), with some exceptions. For example, even though the AWC neurons failed to show their normal pattern of cell fate marker expression, a phenotype that was rescued by re-introducing wild-type copies of *nhr-67* (data not shown), we could not detect expression of *nhr-67* in AWC. This might be due to a non-autonomous role of *nhr-67* or might be a reflection of technical limitations in observing very low levels of *nhr-67* expression. Taken

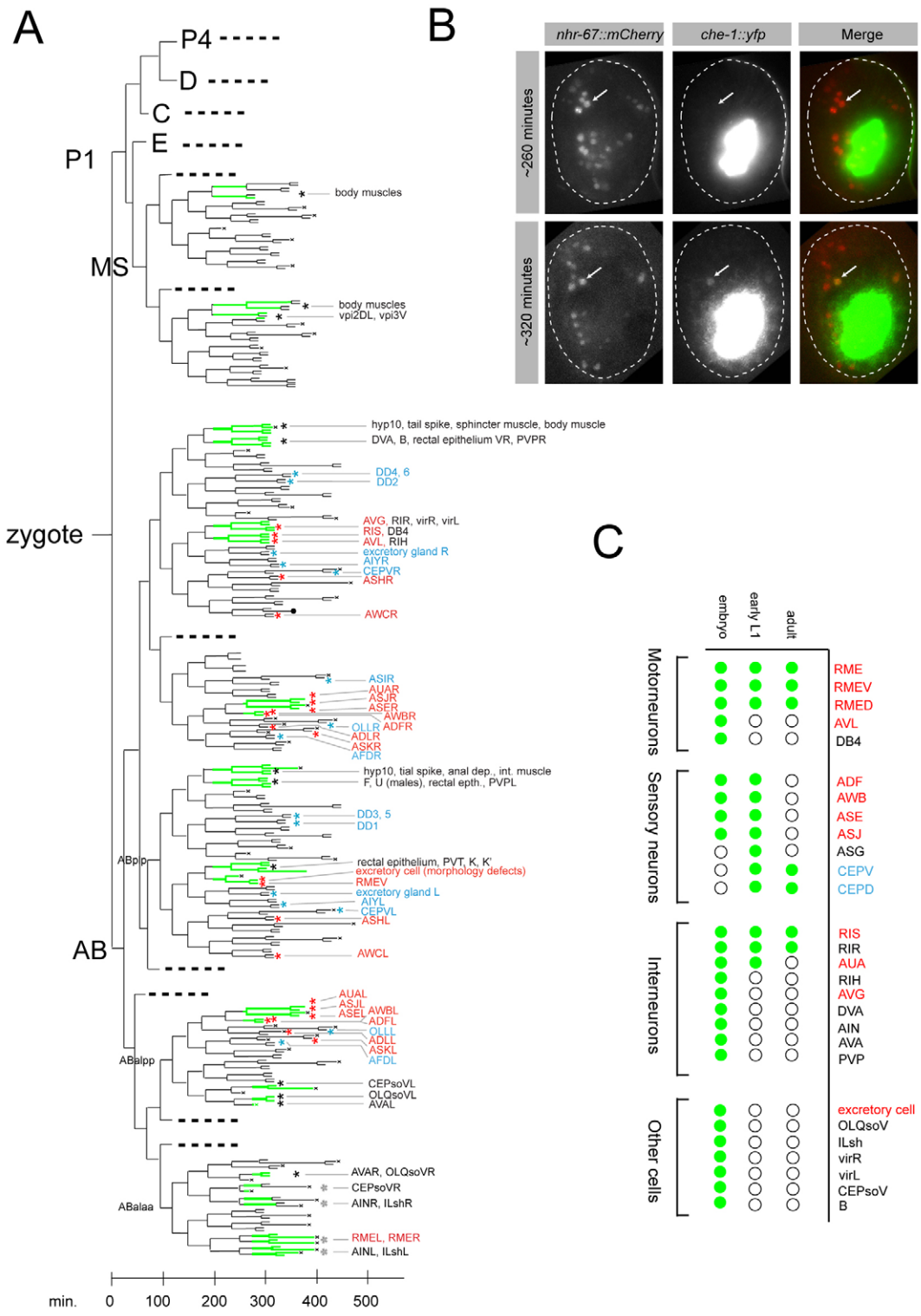

Fig. 6. Expression and function of *nhr-67*. (**A**) Lineage origin of *nhr-67*-expressing cells. *nhr-67* expression is indicated by green lines. Lines begin at the earliest point at which expression was detected within that lineage. Cell identities were determined using 4D microscopy and SIMI software (see Materials and methods). Lineage branches not leading to *nhr-67*-expressing cells are represented by dotted lines. Asterisks denote cells for which we detected (red) or did not detect (blue) defects in fate marker expression in *nhr-67* mutants. Black asterisks denote *nhr-67*-expressing cells for which fate markers were not tested. 'x' indicates apoptotic cell death. (**B**) *nhr-67* is expressed earlier than *che-1* in the ASE lineage. The two rows are pictures of two genotypically identical (*otEx3362*, *otIs188*) embryos; pictures were taken at different developmental stages. First column shows red-filtered fluorescence, second column shows yellow-filtered fluorescence and third column is the merged product. Arrows indicate ASE; minutes indicate time postfertilization at 20°C. The observed temporal expression patterns were confirmed in 14 out of 14 scored embryos. (**C**) *nhr-67* expression (green dots) is transient in some, but maintained in other, cells. Cells shown in A are depicted here. Color coding of cell names is as in A.

together, the mutant phenotypic analysis and the expression pattern analysis both support the notion that *nhr-67* acts in a specific subset of diverse neuron types to control their correct development.

nhr-67 controls ASE asymmetry by directly activating *cog-1* expression

Having identified both the molecular identity and the expression pattern of *nhr-67*, we revisited the question of the bimodal activity of *nhr-67* in ASE development. As *nhr-67* expression precedes and is required for *che-1* expression (but not vice versa), *nhr-67* is likely to activate *che-1* expression, either directly or indirectly. But how does the bilateral expression of *nhr-67* in both ASEL and ASER fit with its function as an ASER fate inducer, which, as we have shown, is genetically required for *cog-1* function? We examined the sequence of the *cog-1* promoter and found a phylogenetically conserved, consensus binding site for Tailless-type orphan nuclear receptor (NR2E motif) (DeMeo et al., 2008; Yu et al., 1994) embedded in between two binding sites for the CHE-1 transcription factor ('ASE motif') that are required to induce *cog-1* expression in ASE (O'Meara et al., 2009) (Fig. 7A). Deletion analysis demonstrated that the NR2E motif is required for the initial, embryonic expression of *cog-1* in ASE (Fig. 7B). Moreover, yeast one-hybrid analysis showed that NHR-67 can directly bind to the *cog-1* promoter and that this binding is dependent on the presence of the NR2E motif (Fig. 7C). The function of NHR-67 as an activator of *cog-1* expression is consistent with the genetic data described above, in which we have shown that *nhr-67* suppresses the *cog-1(ot123)* gain-of-function allele. In this allele, owing to a

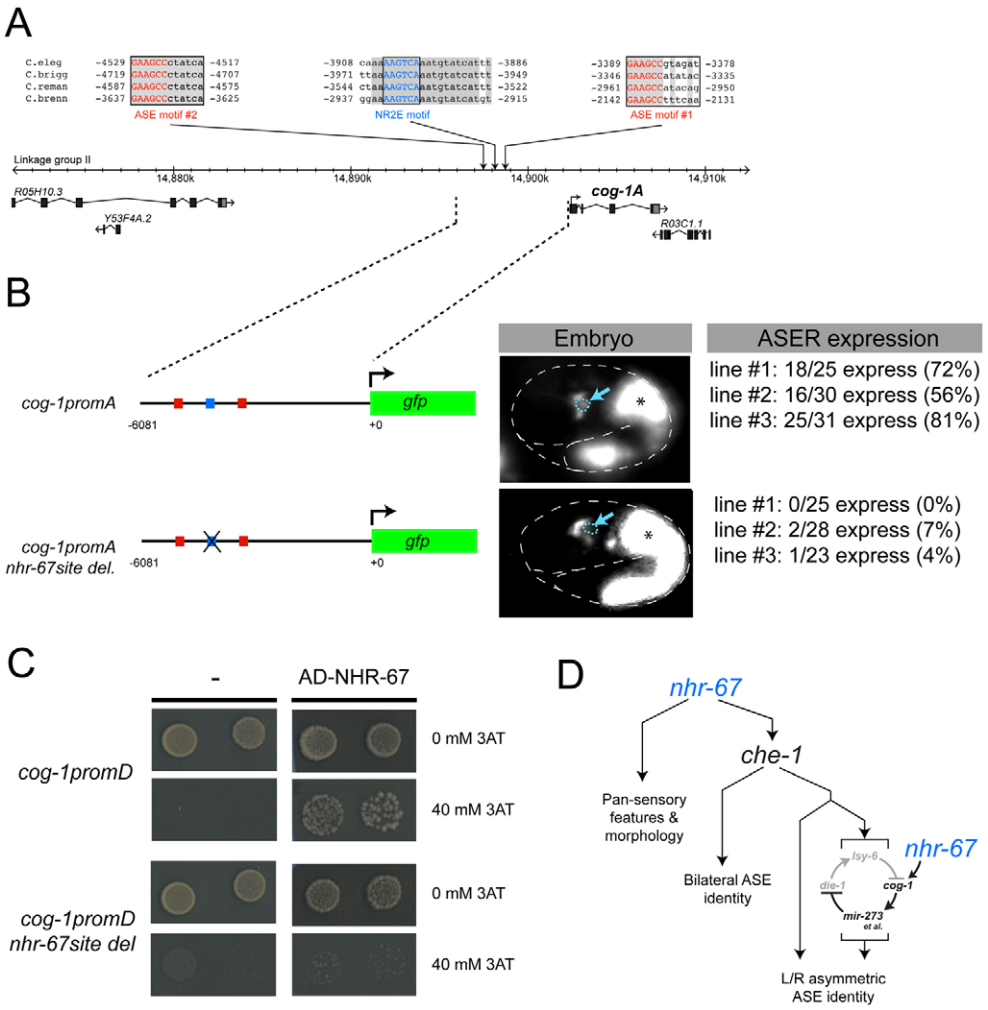

Fig. 7. *nhr-67* controls *cog-1* expression. (**A**) Genomic representation of the intergenic region between *cog-1* and the immediate upstream gene. Numbers next to sequences indicate positions relative to the ATG start codon of the longer *cog-1* isoform. Dotted lines bracket the 6-kb region sufficient to drive *cog-1* expression in ASE (O'Meara et al., 2009). (**B**) Reporter constructs show that the NR2E motif is required for the initiation of *cog-1* expression. Three independent transgenic lines were isolated and scored for each construct in two-fold embryos (when *cog-1* expression is first observed) and in young adults (not shown). Arrows indicate the position of the ASER cell body. Black asterisks indicate intestinal *gfp* expression resulting from the co-injection marker *elt-2::gfp*. Deletion of the NR2E motif does not affect adult expression of *cog-1*, which is likely to be due to *cog-1* autoregulation. (**C**) Yeast one-hybrid interaction between NHR-67 and the *cog-1* promoter. *cog-1promD* is a 1.8-kb fragment of the *cog-1* promoter region that contains the NR2E motif, and *cog-1promD-nhr-67site del* is the same fragment but with the NR2E site deleted. Thirty-two transformants were selected for each transformation and plated on SC –Trp –His with or without 40 mM 3AT. Representatives for each are shown here. All transformants grew on media lacking 3AT. Scoring for strains plated on 40 mM 3AT is as follows: *cog-1promD* alone, 0/32 grew; *cog-1promD* and AD-NHR-67, 25/32 grew; *cog-1promD-nhr-67site del* alone, 0/32 grew; *cog-1promD-nhr-67site del* and AD-NHR-67, 0/32 grew. (**D**) Summary of *nhr-67* function.

deletion of its miRNA-controlled 3′UTR, endogenous *cog-1* is ectopically expressed in ASEL, and its ASER fate-inducing effect in ASEL is dependent on the activation of its transcription by *nhr-67*. Taken together, bilaterally expressed *nhr-67* exerts its function in controlling ASE laterality by activating the ASER fate inducer *cog-1*. This function occurs postmitotically after the birth of the ASE neurons and is subsequent to the earlier role of inducing *che-1* expression, which happens in the mother of ASE.

DISCUSSION

nhr-67 regulates neuronal identity on several different levels

We have delineated here a set of cellular functions of the *C. elegans* Tailless/TLX ortholog NHR-67 in controlling neuronal development. *nhr-67* controls the identity of several different neuronal classes. There is no obvious unifying common theme in the function (sensory versus inter versus motoneurons), neurotransmitter identity, position or morphology of the neurons affected. The cellular fate markers affected by *nhr-67* also tend to be diverse. Some neurons are related by lineage and, based on the *nhr-67* expression pattern, *nhr-67* might affect the identity of the neuroblast from which these affected neurons are derived.

Through their placement in a complex network of regulatory interactions, the ASE gustatory neurons have served as our model to better understand *nhr-67* function (Fig. 7D). We find that *nhr-67* exhibits a unique phenotype characterized by multiple roles in the ASE developmental pathway. In both left and right ASEs, *nhr-67* is required for the induction of ASE fate, as it positively regulates embryonic expression of the ASE selector gene, *che-1*. *che-1* expression is turned on shortly after *nhr-67* expression can be observed in the ASE mother cell, which would be consistent with a direct role of NHR-67 in activating the *che-1* promoter. The *che-1* promoter contains no perfect match to the AAGTCA core binding sequence of TLX-type transcription factors [which was also found to bind NHR-67 in a heterologous yeast system (DeMeo et al., 2008)], but it is possible that NHR-67 might bind to a phylogenetically conserved derivative of this sequence in the *che-1* promoter (cAGTtA), which we find to be required for embryonic induction of *che-1* expression (our unpublished data). The *che-1* promoter also contains several other conserved motifs that are required for the initiation of *che-1* expression (our unpublished data), suggesting that *che-1* integrates several regulatory inputs, of which NHR-67 is likely to be one. The partially penetrant effects of a loss of NHR-67 on *che-1* expression are consistent with other regulatory inputs into the *che-1* locus.

The function of *nhr-67* in controlling the induction of ASE fate extends beyond regulating *che-1* function (Fig. 7D). In *che-1* null mutants, ASE loses its specific neuronal identity, but still persists as a sensory neuron, as indicated by the unaffected expression of ciliated markers and by its overall morphology, as assessed by the ability of ASE to take up the dye DiI and by electron microscopy (Lewis and Hodgkin, 1977; Uchida et al., 2003). By contrast, in *nhr-67* mutants, ASE fails to take up DiI, fails to express a ciliated marker gene and displays morphological defects. Pan-neuronal features of ASE appear to be unaffected by *nhr-67*. These findings reveal a regulatory hierarchy in which *nhr-67* couples the adoption of two identity-defining features of ASE (Fig. 7D). *nhr-67* controls broad, pan-sensory features of ASE, but then also induces the expression of a terminal selector gene that assigns a unique identity to ASE that distinguishes it from other sensory neurons. The *lim-4* LIM homeobox gene is a putative terminal selector of AWB fate (Sagasti et al., 1999), and its regulation by *nhr-67* might indicate that *nhr-67* activity in neuroblasts generally involves the initiation of terminal selector gene expression, which in turn drives the ‘nuts-and-bolts’ gene expression programs that define individual neuron types (Hobert, 2008).

After induction of ASE bilateral fate by promoting *che-1* expression, *nhr-67* plays a further role in inducing ASER and repressing ASEL fate, a decision made long after the birth of the ASE neurons and therefore temporally ‘downstream’ of the earlier role in ASE fate induction in the ASE mother cell. In this additional function, NHR-67 cooperates with the ASE fate-inducer CHE-1; both proteins act through defined cis-regulatory elements to activate the asymmetry regulator *cog-1*, an ASER fate inducer. Bilaterally expressed CHE-1 and NHR-67 transcriptionally activate *cog-1* in both ASEL and ASER, yet COG-1 protein expression is inhibited in ASEL post-transcriptionally by the miRNA *lsy-6* (Johnston and Hobert, 2003). Transcription factors therefore produce a transcriptional program that is refined by miRNA function.

Taken together, *nhr-67* acts at distinct steps in ASE specification. Reiterative uses of a transcription factor in neuronal lineages comparable to the one shown here for *nhr-67* tend to be hard to identify, often because earlier functions of a transcription factor might mask its later roles. It was only through the partial penetrance of the earlier role of *nhr-67* that we were able to uncover its later role. Similarly separable functions of neuronal identity determinants have been described for the *unc-86* homeobox gene and the *lin-32* bHLH gene (Duggan et al., 1998; Portman and Emmons, 2000), and might reflect a common theme of transcription factor activity controlling neuronal development at several distinct steps.

Diverse roles of *nhr-67* and other NR2E nuclear receptors

The function of *nhr-67* is not restricted to the nervous system. In the developing vulva, *nhr-67* controls the identity of several vulval cell types, acting in conjunction with several distinct regulatory factors (Fernandes and Sternberg, 2007). As is the case in the ASE neurons, *nhr-67* acts within the context of a bistable system in which two factors, *cog-1* and *nhr-67*, cross-inhibit the activity of one another to generate distinct vulval cell types. The interaction of *nhr-67* and *cog-1* in ASE neurons is, however, strikingly distinct from the interaction in the vulva, because in ASE *nhr-67* activates *cog-1*, whereas in the vulva it inhibits its expression, presumably because it co-operates with factors other than CHE-1 to control *cog-1* expression. Also, in contrast to in the vulva, *cog-1* has no comparable transcriptional impact on *nhr-67* in ASER. *cog-1* and *nhr-67* therefore are striking examples of regulatory factors wired together in distinct configurations in different cell types.

A nuclear receptor closely related to NHR-67, FAX-1, also controls neuronal identity and morphology in *C. elegans* (Much et al., 2000; Wightman et al., 2005). Similarly, its vertebrate homolog, PNR, promotes proper photoreceptor cell fate specification (Haider et al., 2000). In other species, the orthologs of NHR-67, *Drosophila* Tailless and vertebrate TLX, are also involved in various aspects of neuronal development. Tailless promotes the formation of large regions of the *Drosophila* brain by activating expression of the proneural gene *lethal of scute*, rendering the cells competent to form neural precursors (Strecker et al., 1986; Younossi-Hartenstein et al., 1997). Tailless mutants result in the loss of several brain regions owing to a lack of neuroblast production. Similarly, vertebrate TLX is a key regulator of the cell cycle in neuronal stem cell populations. $Tlx^{-/-}$ mice are unable to maintain an undifferentiated population of stem cells and, consequently, lose several parts of outer brain regions (Miyawaki et al., 2004; Roy et al., 2004; Shi et al., 2004; Stenman et al., 2003). Our finding of NHR-67 acting at several independent steps late in neuronal

differentiation suggests that Tailless-like proteins in other organisms may also have late differentiation roles that might have been obscured by their earlier roles in neuronal precursor formation.

Acknowledgements
We thank M. O'Meara for providing *otIs158* and *ot190*, E. Flowers for *ot247*, V. Marrero for yeast manipulation assistance, M. Walhout for the yeast one-hybrid strain, Q. Chen for expert DNA injection and members of the Hobert lab for comments on the manuscript. We acknowledge funding by the NIH to O.H. (R01NS039996-05, R01NS050266-03) and to S.S. (NS054540-01). B.T. is funded by the Francis Goelet Fellowship. O.H. is an Investigator of the HHMI. Deposited in PMC for release after 6 months.

Supplementary material
Supplementary material for this article is available at
http://dev.biologists.org/cgi/content/full/136/17/2933/DC1

References
Brenner, S. (1974). The genetics of Caenorhabditis elegans. *Genetics* **77**, 71-94.
Buechner, M., Hall, D. H., Bhatt, H. and Hedgecock, E. M. (1999). Cystic canal mutants in Caenorhabditis elegans are defective in the apical membrane domain of the renal (excretory) cell. *Dev. Biol.* **214**, 227-241.
Chang, S., Johnston, R. J., Jr and Hobert, O. (2003). A transcriptional regulatory cascade that controls left/right asymmetry in chemosensory neurons of C. elegans. *Genes Dev.* **17**, 2123-2137.
DeMeo, S. D., Lombel, R. M., Cronin, M., Smith, E. L., Snowflack, D. R., Reinert, K., Clever, S. and Wightman, B. (2008). Specificity of DNA-binding by the FAX-1 and NHR-67 nuclear receptors of Caenorhabditis elegans is partially mediated via a subclass-specific P-box residue. *BMC Mol. Biol.* **9**, 2.
Deplancke, B., Dupuy, D., Vidal, M. and Walhout, A. J. (2004). A gateway-compatible yeast one-hybrid system. *Genome Res.* **14**, 2093-2101.
Dolphin, C. T. and Hope, I. A. (2006). Caenorhabditis elegans reporter fusion genes generated by seamless modification of large genomic DNA clones. *Nucleic Acids Res.* **34**, e72.
Duggan, A., Ma, C. and Chalfie, M. (1998). Regulation of touch receptor differentiation by the Caenorhabditis elegans mec-3 and unc-86 genes. *Development* **125**, 4107-4119.
Durand, B., Saunders, M., Gaudon, C., Roy, B., Losson, R. and Chambon, P. (1994). Activation function 2 (AF-2) of retinoic acid receptor and 9-cis retinoic acid receptor: presence of a conserved autonomous constitutive activating domain and influence of the nature of the response element on AF-2 activity. *EMBO J.* **13**, 5370-5382.
Etchberger, J. F., Lorch, A., Sleumer, M. C., Zapf, R., Jones, S. J., Marra, M. A., Holt, R. A., Moerman, D. G. and Hobert, O. (2007). The molecular signature and cis-regulatory architecture of a C. elegans gustatory neuron. *Genes Dev.* **21**, 1653-1674.
Etchberger, J. F., Flowers, E. B., Poole, R. J., Bashllari, E. and Hobert, O. (2009). Cis-regulatory mechanisms of left/right asymmetric neuron-subtype specification in C. elegans. *Development* **136**, 147-160.
Fernandes, J. S. and Sternberg, P. W. (2007). The tailless ortholog nhr-67 regulates patterning of gene expression and morphogenesis in the C. elegans vulva. *PLoS Genet.* **3**, e69.
Gengyo-Ando, K. and Mitani, S. (2000). Characterization of mutations induced by ethyl methanesulfonate, UV, and trimethylpsoralen in the nematode Caenorhabditis elegans. *Biochem. Biophys. Res. Commun.* **269**, 64-69.
Gissendanner, C. R., Crossgrove, K., Kraus, K. A., Maina, C. V. and Sluder, A. E. (2004). Expression and function of conserved nuclear receptor genes in Caenorhabditis elegans. *Dev. Biol.* **266**, 399-416.
Haider, N. B., Jacobson, S. G., Cideciyan, A. V., Swiderski, R., Streb, L. M., Searby, C., Beck, G., Hockey, R., Hanna, D. B., Gorman, S. et al. (2000). Mutation of a nuclear receptor gene, NR2E3, causes enhanced S cone syndrome, a disorder of retinal cell fate. *Nat. Genet.* **24**, 127-131.
Hobert, O. (2005). Specification of the nervous system. *WormBook*, www.wormbook.org.
Hobert, O. (2006). Architecture of a MicroRNA-controlled gene regulatory network that diversifies neuronal cell fates. *Cold Spring Harb. Symp. Quant. Biol.* **71**, 181-188.
Hobert, O. (2008). Regulatory logic of neuronal diversity: terminal selector genes and selector motifs. *Proc. Natl. Acad. Sci. USA* **105**, 20067-20071.
Hodgkin, J. and Doniach, T. (1997). Natural variation and copulatory plug formation in Caenorhabditis elegans. *Genetics* **146**, 149-164.
Johnston, R. J. and Hobert, O. (2003). A microRNA controlling left/right neuronal asymmetry in Caenorhabditis elegans. *Nature* **426**, 845-849.
Lewis, J. A. and Hodgkin, J. A. (1977). Specific neuroanatomical changes in chemosensory mutants of the nematode Caenorhabditis elegans. *J. Comp. Neurol.* **172**, 489-510.
Miyawaki, T., Uemura, A., Dezawa, M., Yu, R. T., Ide, C., Nishikawa, S., Honda, Y., Tanabe, Y. and Tanabe, T. (2004). Tlx, an orphan nuclear receptor, regulates cell numbers and astrocyte development in the developing retina. *J. Neurosci.* **24**, 8124-8134.
Much, J. W., Slade, D. J., Klampert, K., Garriga, G. and Wightman, B. (2000). The fax-1 nuclear hormone receptor regulates axon pathfinding and neurotransmitter expression. *Development* **127**, 703-712.
O'Meara, M. M., Bigelow, H., Flibotte, S., Etchberger, J. F., Moerman, D. G. and Hobert, O. (2009). Cis-regulatory mutations in the caenorhabditis elegans homeobox gene locus cog-1 affect neuronal development. *Genetics* **181**, 1679-1686.
Ortiz, C. O., Faumont, S., Takayama, J., Ahmed, H. K., Goldsmith, A. D., Pocock, R., McCormick, K. E., Kunimoto, H., Iino, Y., Lockery, S. et al. (2009). Lateralized gustatory behavior of C.elegans is controlled by specific receptor-type guanylyl cyclases. *Curr. Biol.* **19**, 996-1004.
Pierce-Shimomura, J. T., Faumont, S., Gaston, M. R., Pearson, B. J. and Lockery, S. R. (2001). The homeobox gene lim-6 is required for distinct chemosensory representations in C. elegans. *Nature* **410**, 694-698.
Poole, R. J. and Hobert, O. (2006). Early embryonic programming of neuronal left/right asymmetry in C. elegans. *Curr. Biol.* **16**, 2279-2292.
Portman, D. S. and Emmons, S. W. (2000). The basic helix-loop-helix transcription factors LIN-32 and HLH-2 function together in multiple steps of a C. elegans neuronal sublineage. *Development* **127**, 5415-5426.
Roy, K., Kuznicki, K., Wu, Q., Sun, Z., Bock, D., Schutz, G., Vranich, N. and Monaghan, A. P. (2004). The Tlx gene regulates the timing of neurogenesis in the cortex. *J. Neurosci.* **24**, 8333-8345.
Ruvinsky, I., Ohler, U., Burge, C. B. and Ruvkun, G. (2007). Detection of broadly expressed neuronal genes in C. elegans. *Dev. Biol.* **302**, 617-626.
Sagasti, A., Hobert, O., Troemel, E. R., Ruvkun, G. and Bargmann, C. I. (1999). Alternative olfactory neuron fates are specified by the LIM homeobox gene lim-4. *Genes Dev.* **13**, 1794-1806.
Sarin, S., O'Meara, M. M., Flowers, E. B., Antonio, C., Poole, R. J., Didiano, D., Johnston, R. J., Jr, Chang, S., Narula, S. and Hobert, O. (2007). Genetic screens for Caenorhabditis elegans mutants defective in left/right asymmetric neuronal fate specification. *Genetics* **176**, 2109-2130.
Schnabel, R., Hutter, H., Moerman, D. and Schnabel, H. (1997). Assessing normal embryogenesis in Caenorhabditis elegans using a 4D microscope: variability of development and regional specification. *Dev. Biol.* **184**, 234-265.
Shi, Y., Chichung Lie, D., Taupin, P., Nakashima, K., Ray, J., Yu, R. T., Gage, F. H. and Evans, R. M. (2004). Expression and function of orphan nuclear receptor TLX in adult neural stem cells. *Nature* **427**, 78-83.
Sluder, A. E., Mathews, S. W., Hough, D., Yin, V. P. and Maina, C. V. (1999). The nuclear receptor superfamily has undergone extensive proliferation and diversification in nematodes. *Genome Res.* **9**, 103-120.
Stenman, J. M., Wang, B. and Campbell, K. (2003). Tlx controls proliferation and patterning of lateral telencephalic progenitor domains. *J. Neurosci.* **23**, 10568-10576.
Strecker, T. R., Kongsuwan, K., Lengyel, J. A. and Merriam, J. R. (1986). The zygotic mutant tailless affects the anterior and posterior ectodermal regions of the Drosophila embryo. *Dev. Biol.* **113**, 64-76.
Sulston, J. E., Schierenberg, E., White, J. G. and Thomson, J. N. (1983). The embryonic cell lineage of the nematode Caenorhabditis elegans. *Dev. Biol.* **100**, 64-119.
Suzuki, H., Thiele, T. R., Faumont, S., Ezcurra, M., Lockery, S. R. and Schafer, W. R. (2008). Functional asymmetry in Caenorhabditis elegans taste neurons and its computational role in chemotaxis. *Nature* **454**, 114-117.
Swoboda, P., Adler, H. T. and Thomas, J. H. (2000). The RFX-type transcription factor DAF-19 regulates sensory neuron cilium formation in C. elegans. *Mol. Cell* **5**, 411-421.
Tursun, B., Cochella, L., Carrera, I. and Hobert, O. (2009). A toolkit and robust pipeline for the generation of fosmid-based reporter genes in C. elegans. *PLoS ONE* **4**, e4625.
Uchida, O., Nakano, H., Koga, M. and Ohshima, Y. (2003). The C. elegans che-1 gene encodes a zinc finger transcription factor required for specification of the ASE chemosensory neurons. *Development* **130**, 1215-1224.
Wightman, B., Ebert, B., Carmean, N., Weber, K. and Clever, S. (2005). The C. elegans nuclear receptor gene fax-1 and homeobox gene unc-42 coordinate interneuron identity by regulating the expression of glutamate receptor subunits and other neuron-specific genes. *Dev. Biol.* **287**, 74-85.
Younossi-Hartenstein, A., Green, P., Liaw, G. J., Rudolph, K., Lengyel, J. and Hartenstein, V. (1997). Control of early neurogenesis of the Drosophila brain by the head gap genes tll, otd, ems, and btd. *Dev. Biol.* **182**, 270-283.
Yu, R. T., McKeown, M., Evans, R. M. and Umesono, K. (1994). Relationship between Drosophila gap gene tailless and a vertebrate nuclear receptor Tlx. *Nature* **370**, 375-379.
Yu, S., Avery, L., Baude, E. and Garbers, D. L. (1997). Guanylyl cyclase expression in specific sensory neurons: a new family of chemosensory receptors. *Proc. Natl. Acad. Sci. USA* **94**, 3384-3387.
Zheng, X., Chung, S., Tanabe, T. and Sze, J. Y. (2005). Cell-type specific regulation of serotonergic identity by the C. elegans LIM-homeodomain factor LIM-4. *Dev. Biol.* **286**, 618-628.

Table S1. Expression of non-ASE fate markers in *lsy-9*

Cell	*gfp*	Genotype	2 cells (wild type)	1 cell	0 cells	*n*
ASJ	*gpa-9*	Wild type	100%	0%	0%	20
		ot85	85.3%	14.7%	0%	34
		ok631	15%	11%	74%	27
AUA	*flp-8*	Wild type	100%	0%	0%	20
		ot85	76.9%	20.5%	2.6%	39
		ok631	50%	25%	25%	20
AFD	*gcy-8*	Wild type	100%	0%	0%	25
		ot85	100%	0%	0%	44
		ok631	n/a	n/a	n/a	n/a
AWB	*str-1*	Wild type	100%	0%	0%	25
		ot85	78%	22%	0%	50
		ok631	43.8%	47.5%	8.7%	80
	lim-4	Wild type	100%	0%	0%	30
		ok631	70%	20%	10%	30
ASK	*srb-6*	Wild type	100%	0%	0%	25
		ot85	67.3%	22.4%	10.2%	49
		ok631	66.7%	25.9%	7.4%	54
ADL	*srb-6*	Wild type	100%	0%	0%	25
		ot85	87.8%	6.1%	6.1%	49
		ok631	87.0%	13.0%	0%	54
ADF	*srb-6*	Wild type	100%	0%	0%	25
		ot85	40.8%	44.9%	14.3%	49
		ok631	57.4%	25.9%	16.7%	54
	tph-1	Wild type	100%	0%	0%	30
		ok631	7.3%	72.7%	20%	55
		*ok631; lim-4 (yz12); otEx3103**	7.4%	40.7%	51.9%	54
		ok631; lim-4 (yz12)	3.3%	15.6%	81.1%	90
ASH	*srb-6*	Wild type	100%	0%	0%	25
		ot85	81.6%	18.4%	0%	49
		ok631	64.8%	24.1%	11.1%	54
AVG†	*inx-18*	Wild type	n/a	100%	0%	40
		ok631	n/a	6%	94%	36
AWC	*str-2*	Wild type	n/a	98.2%	1.8%	56
		ok631	n/a	59.1%	40.9%	88
ASI	*sra-6*	Wild type	100%	0%	0%	20
		ok631	100%	0%	0%	21
PVQ	*sra-6*	Wild type	100%	0%	0%	20
		ok631	100%	0%	0%	21
AIY	*ttx-3*	Wild type	100%	0%	0%	50
		ok631	100%	0%	0%	28
OLL	*ser-2*	Wild type	100%	0%	0%	30
		ok631	100%	0%	0%	30
RME (D/V/L/R)	*unc-47*	Wild type	100% (4 cells)	0%	0%	30
		ok631	9.1%	72.7% (1-3 cells)	18.2%	44
AVL†	*unc-47*	Wild type	n/a	100%	0%	30
		ok631	n/a	46.7%	53.3%	44
RIS†	*unc-47*	Wild type	n/a	100%	0%	30
		ok631	n/a	36.4%	63.6%	44
D motor neurons	*unc-47*	Wild type	100% (6 cells)	0%	0%	30
		ok631	100% (6 cells)	0%	0%	44
CEPD, CEPV, ADE	*dat-1*	Wild type	100% (6 cells=wild type)	0%	0%	25
		ok631	100% (6 cells=wild type)	0%	0%	31

Red text indicates defects; blue, no defects observed.
**nhr-67(ok631)* is rescued by the presence of the *otEx3103*, *nhr-67*-containing fosmid.
†These cells are unilateral, rendering the first scoring category irrelevant.
n/a, not applicable.